A bi-harmonic five-phase SPM machine with low ripple torque for marine propulsion

Franck Scuiller[1], Hussein Zahr[2], Eric Semail[2]
[1]Ecole Navale; Naval Academy Research Institute, Brest, France, franck.scuiller@ecole-navale.fr
[2]Ecole Nationale Supérieure d'Arts et Métiers; Laboratory of Electrical Engineering and Power Electronics, Lille, France

***Abstract*—This paper addresses the design of a bi-harmonic five-phase Surface-mounted Permanent Magnet (SPM) machine for marine propulsion. The bi-harmonic characteristic results from the particular 20 slots-8 poles configuration that makes possible high value of third harmonic current injection. Thus the machine performance can be improved in terms of average torque, speed range, losses control and torque quality, this last feature being the scope of the paper. As low ripple torques are wanted at low speed, the magnet layer is defined to reduce the cogging torque and to make third harmonic current injection increasing average torque and reducing pulsating torque in the same time. According to a selection procedure based on the numerical simulations of a high number of machines, it appears that designing the rotor with two identical radially magnetized magnet that cover two-third the pole arc allows to reach this goal. Referring to an equivalent three-phase machine, the torque ripple level of the bi-harmonic five-phase machine is more than three times lower, thus being obtained with a simple control strategy that aims at achieving constant currents in the rotating frames. The time simulations of the drive confirm the significant reduction of the speed oscillation, especially at low speed.**

I. Introduction

Multi-phase motors are widely used in electrical marine propulsion for reasons such as reliability, smooth torque and distribution of power [1]. For low power propulsion system (less than 10kW), the power partition constraint results from the low DC voltage (less than 60V) that supplies the drive. Hence increasing the phase number enables to limit the rating of the power electronic components. In addition, compactness objective can be more easily achieved if the phase number is considered as a design parameter. For instance, with five-phase machine, third harmonic current injection can be performed to boost the torque [2], [3]. Regarding the rotor, Permanent Magnet (PM) structure contributes to enhance the power density [4], [5]. Furthermore, Surface-mounted Permanent Magnet (SPM) rotor facilitates the ripple torque mitigation that is of critical importance at low speed. If fractional-slot windings facilitate the reduction of cogging torque for SPM machine [6], they also generate magnetomotive force harmonics that could result in excessive magnet losses. Machine with 0.5 slots per phase and per pole ($s_{pp} = 0.5$) are known to limit this effect [7]. In addition, the slot filling can also be improved with this solution [8]. Therefore the machine here considered is a five-phase machine with 20 slots and 8 poles (20-8-5 configuration) for a marine propeller.

Three-phase machine with 12 slots (12-8-3 configuration) could be chosen but this solution does not provide fault tolerant ability. Furthermore, in [9] where 20-8-5 and 12-8-3 machines are compared for the same design specifications (rated torque, power and external diameters are identical) and the same volume of magnetic materials (magnet, copper and iron), it is shown that the 5-phase configuration makes possible a significant reduction of the magnet losses, according to numerical computations.

20-8-5 configuration is a particular winding distribution in so far as the third harmonic factor (0.98) is higher than the fundamental one (0.57). A machine equipped with this winding can be considered as a bi-harmonic five-phase machine since it inherently offers an electronic pole changing effect [10]. With this characteristic, the efficiency of the machine can be improved for the whole speed range: the possibility of limiting the magnet losses at high speed is shown in [9], [10]. The speed range can be enlarged: this is true for SPM machine [11] but also for Interior PM machine [12].

This paper focuses on a characteristic not yet described for 20-8-5 SPM machine. In [13], it is shown that, for five-phase SPM machine, a quite simple third harmonic current injection can be used to virtually eliminate the pulsating torque. The trouble is, except in case of particular design, the smoother torque is obtained for a lower average torque. The present study shows that, with a proper but quite simple design of the rotor magnet layer, it is possible to inject third harmonic to increase the average torque and to reduce the ripple torque in the same time, which is particularly useful at low speed. The paper will be divided into three parts. The first part introduces the multi-machine decomposition for five-phase SPM machine in order to determine bi-harmonic (first and third) current control strategies. The second part addresses the design of the 20-8-5 machine. A high number of machines are simulated with Finite-Elements Analysis (FEA) in order to select the best solution regarding the ripple torque reduction. To demonstrate the improvement regarding three-phase machines, 12-8-3 machines are also examined. The last part focuses on the time simulation of the drive to preliminary evaluate the possible influence of the current control on the ripple torque and the rotating speed deviation.

II. Multi-machine decomposition of five-phase SPM machine to determine control strategies

A. Multi-machine decomposition of a five-phase machine

If the magnetic saturations and the demagnetization issue are not considered, it can be shown that a star-connected five-

978-1-5090-4281-4/17/$31.00

phase SPM machine behaves as two two-phase virtual machines that are magnetically independent but electrically and mechanically coupled [14]. Furthermore, as the rotor saliency can be neglected with SPM machines, the space harmonics are distributed among the two virtual machines: the virtual machine sensitive to the fundamental is called Main Machine (MM) whereas the other sensitive to the third harmonic is called Secondary Machine (SM). The space harmonics are distributed according to the following law:

- MM is sensitive to 1^{st}, 9^{th}, $(10k \pm 1)^{th}$ harmonics
- SM is sensitive to 3^{rd}, 7^{th}, $(10k \pm 3)^{th}$ harmonics

Actually the virtual machine is a physical reading of the mathematical subspace built on the linear application that describes the phase-to-phase magnetic couplings: this two-dimension subspace is usually represented with $\alpha\beta$-axis circuit in stationary frame or with dq-axis circuit in rotating frame. MM and SM are also characterized by their cyclic inductances that will be of the same order with a tooth-concentrated winding, thus making easier the current regulation of the two virtual machines in case of PWM controlled voltage inverter.

B. Electromagnetic torque calculation

Therefore the five-phase machine electromagnetic torque T is the sum of the torque produced by the Main Machine T_1 and the Secondary Machine T_3. If γ denotes the electrical angle, the following expression is obtained:

$$T(\gamma) = T_1(\gamma) + T_3(\gamma) \tag{1}$$

In case of first and third harmonic current control strategy, MM and SM torques can be expressed as follows:

$$T_1(\gamma) = \frac{5}{2}\epsilon_1 I_1 \cos\theta_1 + t_1(\gamma) \tag{2}$$

$$T_3(\gamma) = \frac{5}{2}\epsilon_3 I_3 \cos\theta_3 + t_3(\gamma) \tag{3}$$

In (2) and (3), ϵ_1 and ϵ_3 are the first and third harmonics of the no-load back-emf (at one rad/s speed), I_1 and I_3 are the first and third harmonics of the current and θ_1 and θ_3 are the current-to-back-emf angles for first and third harmonic respectively. t_1 and t_3 denote the pulsating torques. According to the space harmonic distribution property, the MM pulsating torque $t_1(\gamma)$ results from the interaction of the fundamental of the current with particular back-emf harmonics (1^{st}, 9^{th}, $(10k \pm 1)^{th}$) . The same applies for the SM pulsating torque $t_1(\gamma)$ that results from the interaction of the 3rd harmonic of current with particular back-emf harmonics (3^{rd}, 7^{th}, $(10k \pm 3)^{th}$).

C. Control strategy

At low speed, *Maximum Torque Per Ampere* (MTPA) control is wanted, thus meaning that, for both virtual machines, back-emf and current should be aligned. Thus the current-to-back-emf angles equal zero. Therefore, if r denotes I_3 rms current to I_1 rms current ratio and I_b the rated rms current of the machine (that determines the copper losses), the control strategy can be summarized as follows:

$$\begin{cases} (I_1, \theta_1) = \left(\dfrac{I_b}{\sqrt{1+r^2}}, 0\right) \\ (I_3, \theta_3) = \left(\dfrac{rI_b}{\sqrt{1+r^2}}, 0\right) \end{cases} \tag{4}$$

MTPA is obtained if ratio r equals back-emf ϵ_3 to back-emf ϵ_1 ratio:

$$r_{boost} = \frac{\epsilon_3}{\epsilon_1} \tag{5}$$

With this approach, third harmonic current injection increases the average torque. This strategy is called *h1h3-boost*. With this strategy, the trouble is that the average torque enhancement usually comes with more pulsating torque since the SM pulsating torques t_3 add up to the MM ones t_1.

In [13], a control strategy that aims at using the SM to compensate the pulsating torque of the MM is introduced. This control strategy is called *h1h3-damp*: it consists in choosing a particular ratio r that depends of harmonics 7th, 9th, 11th and 13th of the back-emf, that is calculated in order to eliminate the first harmonic of the pulsating torque.

$$r_{damp} = -\frac{\epsilon_{11} - \epsilon_9}{\epsilon_{13} - \epsilon_7} \tag{6}$$

The limitation of this strategy is that the SM operates as generator to absorb the pulsating torques of the MM, thus reducing the average torque and the efficiency. The two introduced controls (*h1h3-boost* and *h1h3-damp*) can be considered as quite simple control in so far as they aim to regulate constant currents in the dq-frames. In particular, *h1h3-damp* control does not require a time varying d or q current components to mitigate the ripple torques (as in [15]). Therefore the implementation of the control with simple PI controllers can be used since the necessary bandwidth of the controllers does not relate to the frequency of the torque ripple.

III. Machine design

A. Objectives

The present section focuses on the 20-8-5 machine design to make the two strategies *h1h3-boost* and *h1h3-damp* practically similar. Hence third harmonic current injection will increase the average torque and reduce the pulsating torque in the same time. Due to its particular winding, the 20-8-5 machine should be designed to be supplied with first and third harmonic of current at low speed. Therefore the base idea consists in designing the rotor such as third harmonic current injection results in average torque increase (boost effect, see (5)) and pulsating torque reduction (damp effect, see (6)) in the same time. However attention must be drawn to the cogging torque that can be very large for this kind of machine: magnet segmentation is a solution to mitigate the cogging torque. It should be mentioned that a quite simple design is aimed for: simple magnet shape and no rotor or stator skewing. Finally, in order to satisfy the pulsating and cogging torque reduction constraints, solutions where the rotor consists in two

identical radially magnetized magnets are explored. As it can be observed in Fig-1 that illustrates the electromagnetic circuit of the machine over one pole pair, the magnet arc length τ_m has to be chosen as a trade-off between cogging and pulsating torque reduction.

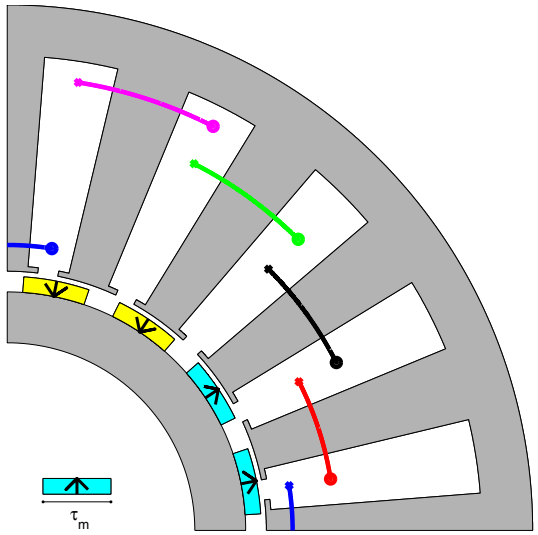

Fig. 1. Machine electromagnetic circuit (for $\tau_m = 1/3$)

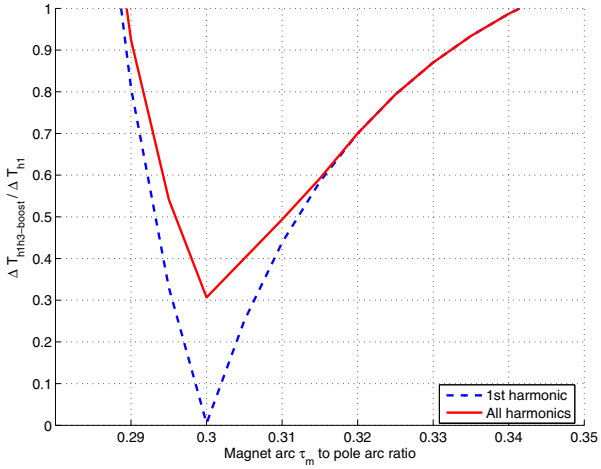

Fig. 2. Magnet arc τ_m for which boost control reduces the pulsating torques (referring to sinus control)

At the pre-design step, the influence of the magnet arc length on the pulsating torque can be analyzed by using an analytical two-dimensional field calculation that allows a quite accurate estimation of the electromagnetic torque [16]. Thus fig-2 shows the variation of the pulsating torque when using boost control (denoted $\Delta T_{h1h3-boost}$, corresponding to (5)) out of the pulsating torque when using sinus control (denoted ΔT_{h1}, obtained by chosing $r = 0$ in (4)) according to the magnet arc length τ_m. The dash line reports $\Delta T_{h1h3-boost}/\Delta T_{h1}$ ratio change when only considering the first pulsating torque harmonic whereas the solid line corresponds to the ratio change when accounting the whole pulsating torque harmonics. According to Fig-2, the boost control has damp effect if the magnet arc length is chosen between 0.29 and 0.34 the pole arc. The main machine parameters are listed in table I.

TABLE I
PARAMETERS FOR THE 5-PHASE MACHINE

Base point	$9.5Nm$ @ $1000rpm$
Pole pair number	$p = 4$
Slot number per phase per pole	$s_{pp} = 0.5$
Effective length	$L_m = 0.050m$
Stator Diameter	$2R_s = 0.100m$
Stator yoke thickness	$t_{ys} = 0.010m$
Mechanical airgap	$g = 0.001m$
Rotor yoke thickness	$t_{yr} = 0.010m$
Magnet layer thickness	$h_m = 3g$
Remanent flux density	$B_r = 1.17T$
Slot width (τ_s, tooth pitch)	$0.5\tau_s$
Slot width opening	$0.25\tau_s$
Slot-closing thickness	$t_{sc} = 0.002m$
Slot depth	$d_s = 0.0405m$

B. Design exploration

In this part, the best design is found by using a numerical two-dimensionnal field calculation (Finite Elements Analysis FEA software *FEMM*, [17]). The advantages of the investigated 20-8-5 machine has to be discussed with regards to an equivalent 12-8-3 machine (with the same rotor diameter, magnet height and air gap).

Usually the rotor of 12-8-3 machine is made with a single magnet per pole that covers two-third the pole pitch. For the considered design specifications, according to FEA, such a machine presents an excessive torque ripple: the peak cogging torque is about 2.2Nm and the max-to-min full torque with MTPA sinus control strategy is higher than 4.5Nm (that is mostly 50% the rated torque). Consequently, skewing the rotor or the stator would be necessary to mitigate the cogging torque, thus making the manufacturing more complex. Controlling the currents to mitigate the cogging torque is possible but more complex and less robust than simply achieving constant currents in the dq-frame. Finally, the investigated 20-8-5 machines with two magnets per pole is compared with an equivalent 12-8-3 one, thus meaning that the equivalent 3-phase machine is also equipped with a rotor made with two identical radially magnetized magnets per pole.

Practically, by varying the pole arc to pole pitch ratio τ_m from 0.25 to 0.49 by 0.01 step, 25 3-phase and 25 5-phase machines are computed: for each of them, no-load and load torques (9.5Nm) are calculated and recorded. Whatever the magnet arc length is, the stator current is modified to make the machine produce the rated average torque (the impact on the thermal and inverter designs is not examined since the goal is finding the less ripple torque solution). For the 3-phase machine, sinus MTPA current control is supposed whereas, for the 5-phase one, three current control strategies are computed:

- the MTPA *h1h3-boost* control introduced by eq.(5)
- the fundamental sinus current control (*h1*, all the torque is produced by the MM, using the 4-pole polarity)

- the third harmonic current control (*h3*, all the torque is produced the SM, using the 3×4-pole polarity).

Fig-3a represents the peak cogging torque change according to the magnet arc length τ_m. One can observe that the peak cogging torque can be minimized by choosing τ_m equal to 0.33 for the 5-phase machine and by choosing τ_m equal to 0.36 for the 3-phase one: nevertheless, according to the FEA predictions, the minimum cogging torque for the 5-phase machine is about two times lower than the 3-phase machine one. This can be explained by lower slot openings for the 5-phase machine.

Fig-3b focuses on the pulsating torque change with magnet arc length τ_m for the 12-8-3 and 20-8-5 machines. The pulsating torque can be reduced up to about 0.6Nm with the 3-phase machine if the magnet arc length is 0.42 the pole pitch. It can be observed that the possible pulsating torque reduction is significantly better with the 5-phase machine: in case of *h1h3-boost* control, a magnet arc length equal to 0.32 the pole pitch corresponds to a pulsating torque of about 0.2Nm (that is three times lower that the best 12-8-3 solution). For 20-8-5 machine, it is worth mentioning that the *h1h3-boost* control reduces the pulsating torques referring to *h1* control if the magnet arc length is between 0.29 and 0.40 the pole pitch, which is quite compliant with the analytical predictions reported in Fig-2. Furthermore, with regards to *h3* control, the resulting pulsating torques are always reduced with the *h1h3-boost* control if the magnet arc length is higher than 0.3 the pole pitch. Finally, according to the numerical predictions, the boost control has a damp effect if the magnet arc length is between 0.3 and 0.4 the pole pitch.

Fig-3c reports the full ripple torque (cogging and pulsating) for the 3-phase and 5-phase machines. As in Fig-3b, 5-phase machine ripple torque is estimated for three current control strategies: *h1h3-boost*, *h1* and *h3*. First, one can observe that the best torque ripple reduction is obtained for the 20-8-5 machine with *h1h3-boost* control: if the magnet pole arc is 0.33 the pole pitch, the max-to-min ripple torque is about 0.5Nm that is more than four times lower the value obtained with the best 12-8-3 machine (about 2.2Nm, corresponding to $\tau_m = 0.39$). In addition, if the analysis is restricted on the 5-phase machine, Fig-3c clearly shows that such a ripple torque reduction can not be obtained with *h1* or *h3* controls. For these two controls, the best result is obtained for *h1* current control applied to a machine with $\tau_m = 0.44$: the ripple torque is then about 1Nm, that is two times the best values ($\tau_m = 0.33$ with *h1h3-boost* control).

C. Results

The final design is the 20-8-5 machine with magnet length equals one-third (0.33) the pole arc. The resulting electromagnetic circuit is depicted in Fig.1. It is worth mentioning that the final 5-phase machine has the same magnet volume as the usual 12-8-3 one (with a single magnet per pole covering two-third the pole pitch), examined at the beginning of subsection III-B.

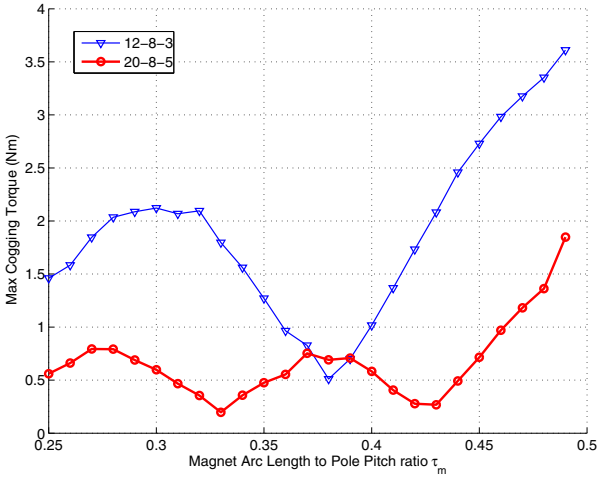

(a) Peak cogging torque change with τ_m

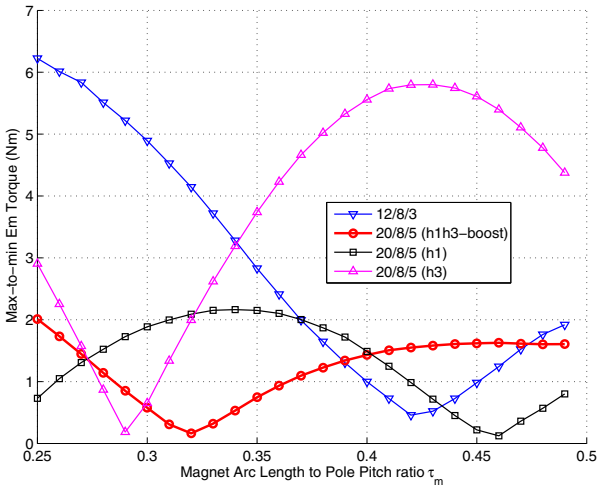

(b) Max-to-min eletromagnetic torque change with τ_m

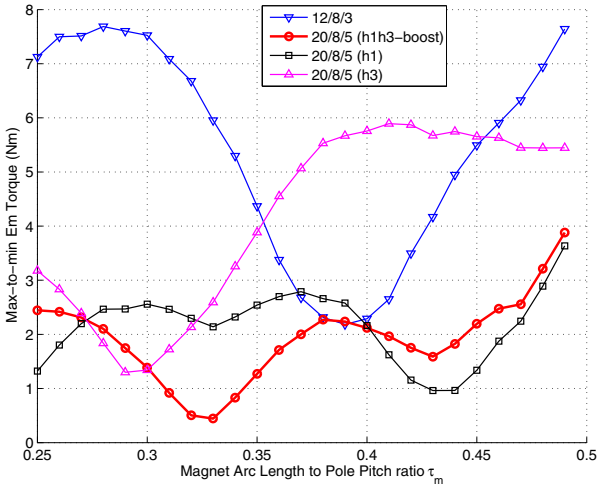

(c) Max-to-min full torque change with τ_m

Fig. 3. Magnet pole arc choice with regard to ripple torque

Fig-4 reports the numerical torque estimations for the best 3-phase machine (with two magnets per pole, obtained for $\tau_m = 0.39$) and the final 5-phase machine: the torque ripple reduction (more than four times) with the 5-phase machine is then illustrated, thus confirming the results in Fig-3c.

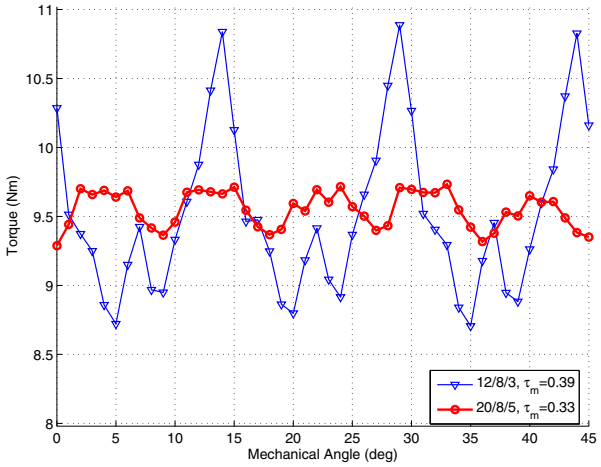

Fig. 4. Torques (FEA) obtained for the best 3-phase machine (sinus current) and the final 5-phase machine (*h1h3-boost* current)

Fig-5 gives the no-load back-emf waveform and the corresponding spectrum for the optimal 20-8-5 machine. It can be observed that the back-emf spectrum contains only four significant terms: 1st and 9th harmonics that belong to the MM space harmonic family on the one hand, 3rd and 7th harmonics that belong to the SM space harmonic family on the other hand. 1st and 3rd harmonic terms are practically equal, thus justifying the bi-harmonic denomination for the here designed 20-8-5 machine. In addition, as 7th and 9th harmonic terms are also practically equal, it can be easily demonstrated by using (5) and (6) that boost and damp controls are virtually the same, which is a very interesting feature:

$$r_{boost} \approx r_{damp} \tag{7}$$

Fig-6 shows the no load back-emf Park components: 1-d and 1-q are the Park components of the Main Machine (the frame rotating at $p\omega_s$rad/s) and 3-d and 3-q are the Park components of the Secondary Machine (the frame rotating at $3p\omega_s$rad/s). The considered control strategies (boost and damp) provide reference Park currents that are constant: 0 for the two 1-d and 3-d currents and 1-q and 3-q references are calculated according to (4). For the designed 20-8-5 machine, the average values of the 1-q and 3-q are almost equal, which complies with the back-emf spectrum analysis. Furthermore, the time-variable parts of the 1-q and 3-q back-emf components are slightly of the same order and in opposition. This property explains why controlling MM (h1) and SM (h3) at the same time allows to reduces the pulsating torques and increase the average torque.

Fig.7 clearly illustrates this property. For the 5-phase machine, the FEA torque estimations with the three possible

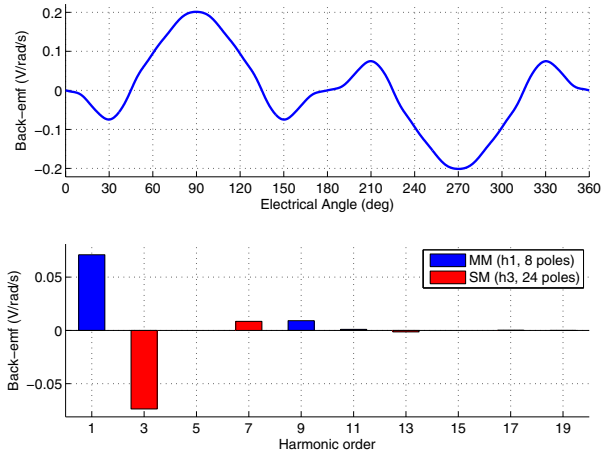

Fig. 5. No load back-emf waveform and spectrum at one rad/s mechanical speed for the 20-8-5 machine (FEA estimation)

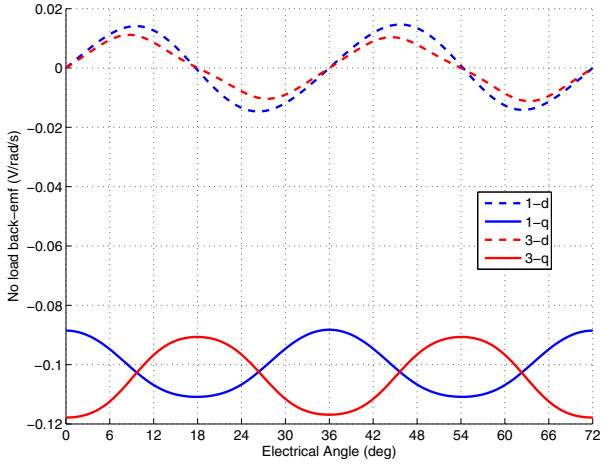

Fig. 6. No-load back-emf Park components (at 1 rad/s mechanical speed, FEA)

control strategies are shown: *h1h3-boost*, *h1* and h3. As during the selection process described in the previous subsection, the average torques are the same. Therefore, when using *h1* or *h3* current control strategy, the required RMS current is higher than the base current that is defined for *h1h3-boost* control strategy: 1.44pu for *h1* and 1.38pu for *h3*. It should be noted that these current values difference is consistent with the slight amplitude deviation between the average 1-q and 3-q back-emf components (visible in Fig-6). It is also worth mentioning that, with these two controls (*h1* and h3), the resulting ripple torques are almost equal to the one obtained with the best 12-8-3 machine (whereas *h1* and *h3* controls are not the proper control for the optimal 20-8-5 machine). Fig.7 shows that the ripple torques with *h1* control and *h3* control are practically in opposition, thus justifying the significant ripple mitigation with *h1h3-boost* control.

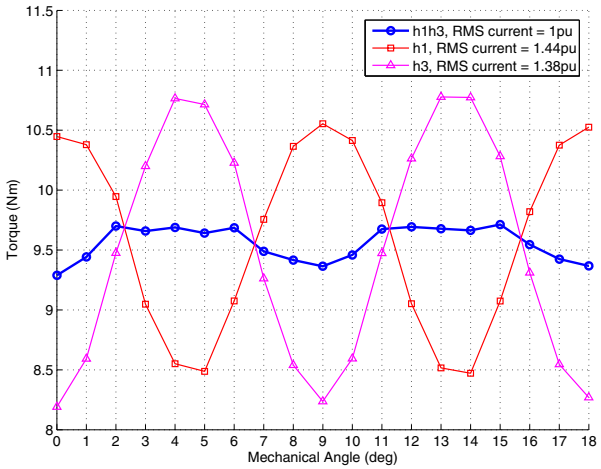

Fig. 7. FEA torque estimations for 20-8-5 machines with the three evaluated controls (*h1*, *h3* and *h1h3-boost*)

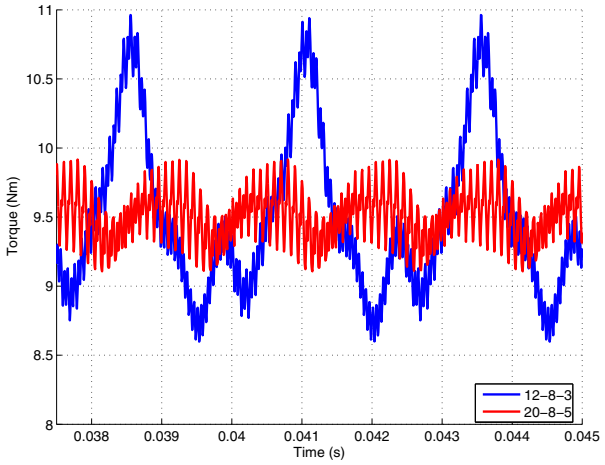

Fig. 8. 3-phase and 5-phase machine torques according to the simulation of the drive at the rated point

IV. Drive Simulations

A. Hypotheses

This subsection addresses the inverter simulation issue in order to evaluate the effects of the real time control of the currents. A time simulation of the drive is thus realized (with *Matlab/Simulink* software) for the best 12-8-3 machine (the one with $\tau_m = 0.39$) and the optimum 20-8-5 machine ($\tau_m = 0.33$). The following hypotheses are taken:

- the inverter is made with perfect switches and the DC bus voltage continuously equals 60V
- an intersective modulation based on a carrier signal at 10kHz is considered
- dq-axis currents (classical dq-axis currents for the 3-phase machine and d_1q_1-axis (MM) and d_3q_3-axis (SM) for the 5-phase machine) are regulated with PI controllers tuned according to [18] with back-emf compensation
- the mechanical load increases with the square of the rotating speed (such as, at full speed, the load torque is the rated machine torque)
- the rotating speed is not regulated.

For both machines, the simulation model accounts the cogging torque. It should be remembered that all the considered current controls aim at achieving constant d-axis (zero) and q-axis currents at steady state (this is the case for the sinus control of the 12-8-3 machine and for the *h1h3-boost*, *h1* and *h3* controls of the 20-8-5 machine).

B. Results

Fig.-8 shows the resulting torque waveforms for the 12-8-3 and 20-8-5 machines according to the simulation of the drives (in steady state). The torque ripple reduction with the 5-phase machine is about three times which complies with the FEA results given in Fig-4. For the 5-phase machine, Fig.-9 reports the d_1q_1-axis and d_3q_3 currents: it can be observed that the currents are virtually constant, thus demonstrating the quite simple control approach to eliminate the ripple torques.

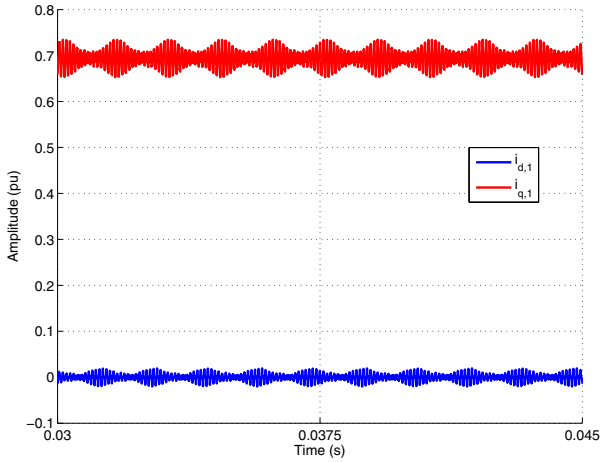

(a) Main Machine d_1 and q_1 currents

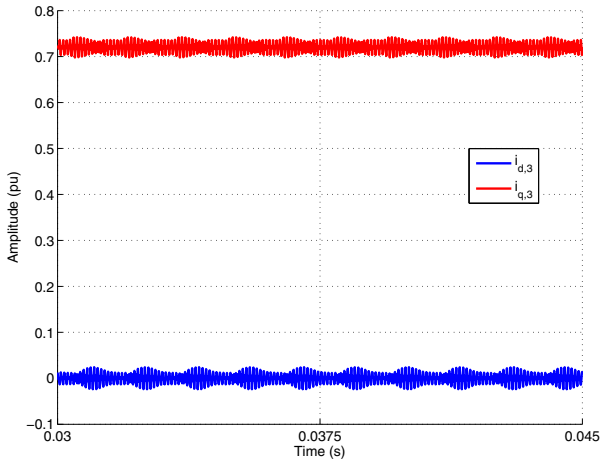

(b) Secondary Machine d_3 and q_3 currents

Fig. 9. d_1q_1-axis d_3q_3 currents for the 5-phase at the rated point

Fig.-10 reports the rotating speed changes for the 3-phase and 5-phase machines, at the rated point (1000rpm, in Fig-10a) and at low speed (250rpm, in Fig-10b). The significant speed oscillation reduction is then illustrated. In particular, at low speed (250rpm), the difference between the maximum speed and the minimum speed is about 70 times lower with the 20-8-5 machine (against 8 times at 1000rpm).

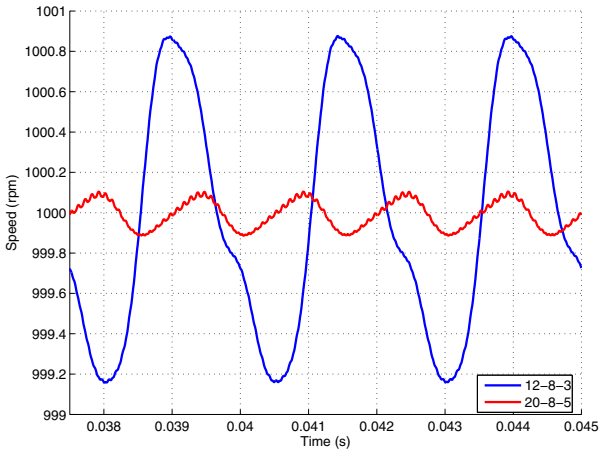

(a) At 1000rpm speed

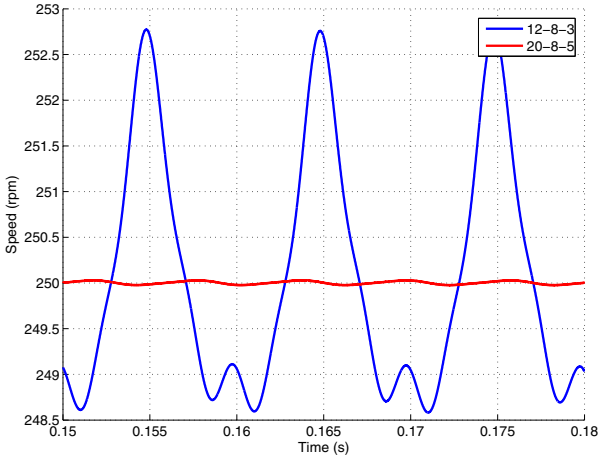

(b) At 250rpm speed

Fig. 10. 3-phase and 5-phase machine rotating speeds according to the simulation of the drive

V. Conclusion

This paper addresses the design of a bi-harmonic five-phase SPM machine for marine propulsion. As low ripple torques are wanted at low speed, the magnet layer is defined to reduce the cogging torque and to make third harmonic current injection increasing average torque and reducing pulsating torque in the same time. Designing the rotor with two identical radially magnetized magnets that cover two-third the pole arc appears as a possibility to reach this goal. Numerical simulations of the five-phase machine confirm this approach and show a significant torque quality improvement: referring to an equivalent three-phase machine, the torque ripple level is reduced by more than three times. The possibility to eliminate the ripple torques with a simple control that aims at achieving constant currents in the rotating frames is evaluated with a time simulation of the drive. For the bi-harmonic five-phase machine, the FEA torque ripple reduction is confirmed and the speed oscillation is significantly mitigated, especially at low speed.

References

[1] E. Levi, "Multiphase electric machines for variable-speed applications," *Industrial Electronics, IEEE Transactions on*, vol. 55, no. 5, pp. 1893–1909, 2008.

[2] E. Semail, X. Kestelyn, and A. Bouscayrol, "Right harmonic spectrum for the back-electromotive force of an n-phase synchronous motor," in *Industry Applications Conference, 2004. 39th IAS Annual Meeting. Conference Record of the 2004 IEEE*, vol. 1, Oct 2004, p. 78.

[3] K. Wang, Z. Zhu, and G. Ombach, "Torque improvement of five-phase surface-mounted permanent magnet machine using third-order harmonic," *Energy Conversion, IEEE Transactions on*, vol. 29, no. 3, pp. 735–747, Sept 2014.

[4] "Oceanvolt website," http://oceanvolt.com, accessed: 2016-29-09.

[5] "Torqeedo website," http://www.torqeedo.com, accessed: 2016-29-09.

[6] Z. Q. Zhu and D. Howe, "Influence of design parameters on cogging torque in permanent magnet machines," *IEEE Transactions on Energy Conversion*, vol. 15, no. 4, pp. 407–412, December 2000.

[7] B. Aslan, E. Semail, and J. Legranger, "General analytical model of magnet average eddy-current volume losses for comparison of multi-phase pm machines with concentrated winding," *Energy Conversion, IEEE Transactions on*, vol. 29, no. 1, pp. 72–83, March 2014.

[8] A. M. EL-Refaie, "Fractional-slot concentrated-windings synchronous permanent magnet machines: Opportunities and challenges," *IEEE Transactions on Industrial Electronics*, vol. 57, no. 1, pp. 107–121, Jan 2010.

[9] H. Zahr, E. Semail, and F. Scuiller, "Five-phase version of 12slots/8poles three-phase synchronous machine for marine-propulsion," in *Vehicle Power and Propulsion Conference (VPPC), 2014 IEEE*, Oct 2014, pp. 1–6.

[10] H. Zahr, F. Scuiller, and E. Semail, "Five-phase spm machine with electronic pole changing effect for marine propulsion," in *ESARS ITEC - 4th International Conference on Electrical Systems for Aircraft, Railway, Ship propulsion and Road Vehicles and International Transportation Electrification Conference*, Nov 2016.

[11] F. Scuiller, H. Zahr, and E. Semail, "Maximum reachable torque, power and speed for five-phase spm machine with low armature reaction," *IEEE Transactions on Energy Conversion*, vol. 31, no. 3, pp. 959–969, Sept 2016.

[12] H. Zahr, E. Semail, B. Aslan, and F. Scuiller, "Maximum torque per ampere strategy for a biharmonic five-phase synchronous machine," in *2016 International Symposium on Power Electronics, Electrical Drives, Automation and Motion (SPEEDAM)*, June 2016, pp. 91–97.

[13] F. Scuiller, "Third harmonic current injection to reduce the pulsating torque of a five-phase spm machine," in *Industrial Electronics Society, IECON 2015 - 41st Annual Conference of the IEEE*, Nov 2015, pp. 000 811–000 816.

[14] E. Semail, A. Bouscayrol, and J.-P. Hautier, "Vectorial formalism for analysis and design of polyphase synchronous machines," *Eur. Phys. J.*, vol. AP 22, pp. 207–220, 2003.

[15] N. Nakao and K. Akatsu, "Suppressing pulsating torques: Torque ripple control for synchronous motors," *Industry Applications Magazine, IEEE*, vol. 20, no. 6, pp. 33–44, Nov 2014.

[16] A. B. Proca, A. Keyhani, A. El-Antably, W. Lu, and M. Dai, "Analytical model for permanent magnets motors with surface mounted magnets," *IEEE Transactions on Energy Conversion*, vol. 18, no. 3, pp. 386–391, September 2003.

[17] D. Meeker, "Finite element method magnetics, version 4.2, users manual," FEMM official website, October 2010.

[18] M. Kamierkowski, R. Krishnan, and F. Blaabjerg, *Control in Power Electronics: Selected Problems, chapter 4*, ser. Academic Press series in engineering. Academic Press, 2002.